

# Effect of Collector Tilt and Orientation on Performance of Adsorption Solar Cooling System

Aro-Zo F.R. Andrianaharinjaka<sup>1,\*</sup>, Vincent Sambou<sup>2</sup>, Modeste K.Nematchoua<sup>3</sup>, Charlain J.N. Keou<sup>3</sup>

<sup>1</sup>Laboratoire de Thermique Appliquée, ESP, Université d'Antsirana, MADAGASCAR

<sup>2</sup>CIFRES, ESP, Université Cheikh Anta Diop, Dakar SENEGAL

<sup>3</sup>Environmental Energy Technologies Laboratory, University of Yaoundé I, Cameroon

Corresponding Email : andriarozo@gmail.com

**Abstract:** A solar cooling system can contribute to saving energy and protecting the environment. This paper investigates the influence of tilt and orientation angles of the collector of an intermittent adsorption cooling system. We are interested in the dynamic behavior and the performance of the system under the climatic conditions of Mahajanga city in Madagascar. The heat and mass transfer into the adsorbent bed was modeled. The results showed that the optimal collector tilts vary from 0 to 45° between June and October. It is also observed that an orientation of the collector towards the sunset increases the specific cooling production and the performance.

**Keywords:** collector, tilt, orientation, solar cooling, adsorption, simulation

## I. Introduction

For over a decade, global warming has increased the need for refrigeration and air conditioning and has led to an overconsumption of electrical energy. On the other hand, the use of certain refrigerants contributes to the depletion of the ozone layer. Thus, one of the solutions suggested is the use of solar energy for cooling. In fact, the cooling demand grows with the level of solar irradiation. This technology should limit energy consumption in urban refrigeration, support the preservation of foodstuffs in rural areas, and preserve medicines in landlocked areas.

A solar adsorption cooling system exploits the interaction between a refrigerant fluid and an adsorbent material to produce cold. The machine does not contain any moving mechanical components. This considerably reduces maintenance costs and allows silent operation. The barriers to large-scale commercialization of these machines are their intermittent operation, low performance and high prices. Thus, several efforts have been made to improve the system. One can refer to the following works: the selection of the best adsorbent/adsorbate pairs; the optimization of operating temperatures and the adsorbent mass; the heat and mass recovery; the hybridizations; and the multiplication of the number of adsorption bed.

The performance of the machine depends essentially on the heating-desorption phase. Various studies have been carried out with this in mind. Chekirou et al. [i] have studied the optimum dimensions of the adsorption bed. Tashtoush et al. [ii] simulated the effect of heating the bed from the inner tube using a heat pipe. Al Mers et al. [iii] have used internal fins in the adsorber.

In addition, several case studies have been carried out, given the dependence of the performance on climate: Alam et al. [iv] have studied the system under the climatic conditions of Tokyo, Japan with 15 collectors of 2.415 m<sup>2</sup> each. They have obtained a cyclic average cooling capacity of 10kW and a SCOP of around 0.3. The influence of cycle time has been observed. Qasem et al. [v] have analyzed the performance of a solar icemaker in the winter and summer seasons for the city of Dhahran, Saudi Arabia. The results have shown a SCOP value between 0.077 and 0.17. Allouhi et al. [vi] have carried out a comparative study of the machine performance for four sub-Saharan African cities. The best specific power and SCOP values found was 3.18 W/kg and 0.132 respectively. The conclusion was drawn that climatic conditions significantly affect the dynamic behavior of the adsorber as well as the system's overall performance.

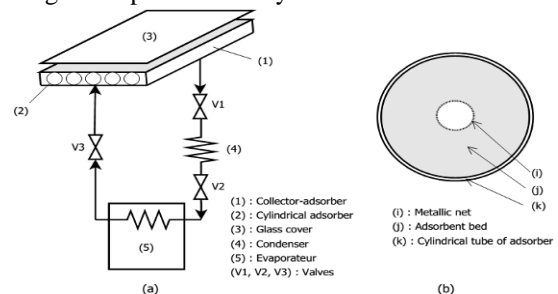
Collector tilt and orientation are additional factors to consider when maximizing performance.

The objective of this paper is to show the influence of the tilt and also that of the orientation of the collector on the system performance. This is done with the use of climatic data of Mahajanga, a city of Madagascar. A numerical model of the transient behavior of the adsorber was used to achieve this objective.

## II. Material and Methodology

### 2.1 System description

The system consists of the main elements shown in Figure 1a. A collector-adsorber (1), a condenser (4), an evaporator (5) and valves (V1,V2,V3) are connected in series. The collector-adsorber consists of cylindrical tubes (2) containing an activated carbon AC-35 (Figure 1b). It is covered by a transparent glass (3) to reduce convection losses and to improve radiation heat transfer. Methanol circulates in the circuit and changes state according to the phase of the cycle.



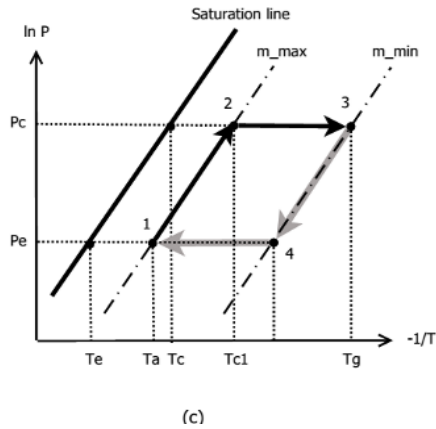


**Fig. 1.** (a) System components (b) Description of the adsorber (c) Cooling cycle diagram

The system operates with an intermittent cycle described in the Clapeyron diagram of Figure 1c. The operating cycle [i] can be summarized in the following four phases (figure 1c): Phase 1 consists of heating and increasing the pressure at constant masse, corresponding to the passage from point 1 to 2; Phase 2 consists of desorption phase at the condenser pressure (Pc) (point 2 to 3); Phase 3 consists of cooling and decreasing the pressure at constant mass, (point 3 to 4); Phase 4 is the adsorption phase at evaporator pressure (Pe) (point 4 to 1). The “black” and “gray” colors of the arrows represent the “day” and “night” phases, respectively.

## 2.2 Mathematical modeling

The heat and mass transfer equations at the adsorbent bed is used to describe the transient behavior of the system. This model makes it possible to determine the duration of each phase of the cycle, the Specific Cooling Production (SCP) and the Solar Coefficient of Performance (SCOP). Thus, some assumptions are necessary:

- The adsorbent bed is assimilated to a continuous and isotropic medium
- The heat transfer in the adsorbent bed is radial
- The pressure in the adsorber is uniform at all points
- The condenser and the evaporator are ideal
- The condensation temperature is equal to the ambient temperature

The adsorbed fraction  $x$  of adsorbent depends on the equilibrium temperature  $T$ , the pressure  $P$ , and the characteristic of the adsorbent/adsorbate pair. Dubinin-Astakhov model (D-A) adequately describe the adsorption isotherms with minimal input data (Equation (1)).

$$x = w_0 \rho_l(T) \exp \left[ -D \left( T \ln \frac{P_s(T)}{P} \right)^n \right] \quad (1)$$

$\rho_l(T)$  represents the density of the liquid adsorbate at the temperature  $T$ ;  $w_0$ ,  $D$  and  $n$  are characteristic parameters of the

adsorbent/adsorbate pair [vii],  $P_c$  and  $P$  are the saturated pressure and pressure of the adsorbate, respectively.

Taking into account the above assumptions, the combined equation of heat and mass transfer is written as follows:

$$\rho_2 \left( Cp_2 + mCp_1 + \frac{bq_{st}^2}{RT^2} \right) \frac{\partial T}{\partial t} = k \left( \frac{\partial^2 T}{\partial r^2} + \frac{1}{r} \frac{\partial T}{\partial r} \right) + \rho_2 bq_{st} \frac{d \ln P}{dt} \quad (2)$$

in which

$$b = nDmT^n \left( \ln \frac{P_s(T)}{P} \right)^{n-1} \quad (3)$$

The different terms of equation 2 represent, respectively, (i) the thermal energy for heating adsorbent bed, (ii) the heat exchanged by conduction, and (iii) heat of adsorption.

The heat balance of external tube is written as follow:

$$C_w \rho_w V_w \frac{\partial T}{\partial t} = 2\tau_v \alpha_w G(t) R_3 L_t - \pi U_L R_3 L_t (T_w - T_{amb}) - 2h\pi R_2 L_t (T_w - T_{r=R_2}) \quad (4)$$

The different terms of this expression represent, respectively, (i) the thermal energy for the heating tube, (ii) solar energy received, (iii) the heat lost to the ambient air, and (iv) the heat transferred to the adsorbent bed. The heat loss coefficient,  $U_L$ , is determined by an empirical relation [viii]. The heat transfer condition between the external tube and the adsorbent bed is expressed by:

$$h(T_w - T_{r=R_2}) = k \frac{\partial T}{\partial r} \Big|_{r=R_2} \quad (5)$$

The inner wall is subjected to a symmetry condition, which is expressed as follows:

$$\frac{\partial T}{\partial r} \Big|_{r=R_1} = 0 \quad (6)$$

The specific cooling production (SCP) is the ratio between the cold production and the cycle time. Its can obtained by the following relation:

$$SCP = \frac{\Delta x \left[ L(T_c) - \int_{T_c}^{T_e} C_{pl}(T) dT \right]}{t_{cycle}} \quad (7)$$

The solar coefficient of performance is the ratio between the cold production  $Q_f$  and the total solar energy captured by the

collector. It is given by this expression in which A represents the total surface area of the collector:

$$SCOP = \frac{Q_f}{\int_{sunrise}^{sunset} A.G(t)dt} \quad (8)$$

### 2.3 Numerical resolution

The above equations were solved numerically by an implicit finite difference method with MATLAB. The non-linearity of the equation was resolved by an iterative procedure. The model was validated with the results in the literature [i]. The hourly ambient temperature, the average daily wind speed and the hourly global real-sky irradiation on an inclined plane was provided by HelioClim-3 [ix] and MERRA-2 [x] for Mahajanga (15°42'S, 46°18'W) in 2005.

## III. Results and discussions

### 3.1 Effect of the collector tilt

Figure 3 illustrate the influence of the collector tilt on the SCP and the SCOP. Simulations were carried out for tilt varying from 0 to 60° in increments of 10° and the orientation fixed to the north. Figure 3a and figure 3b show the results for October 21<sup>st</sup> and June 21<sup>st</sup>, respectively.

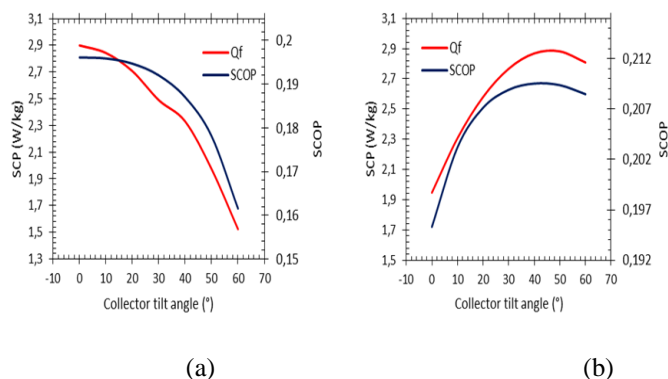


**Fig. 2.** Effect of collector tilt on SCP and the SCOP on (a) October 21<sup>st</sup> and (b) June 21<sup>st</sup>

We observe in these figures that SCP and SCOP vary together in the same direction. In the figure 3a, SCP and the SCOP decrease when the collector tilt is increased. They decrease respectively by 47% and 10% for a collector tilt between 0 and 45°. The maximum values are 2.9 W/kg and 0.196, respectively, and are obtained when the collector tilt is 0°. Figure 2b shows an inverse evolution. Indeed, SCP and the SCOP increase with increasing collector tilt and reach maximum values before decreasing. For a collector tilt between 0 and 45°, SCP and the SCOP increase by 32% and 6%, respectively. These maximum values are 2.88 W/kg and 0.209, respectively, and are obtained when the collector tilt is 45°.

We notice that all the maximum values above were obtained when the collector tilt approximately follows the azimuthal position of the sun. Indeed, the sun azimuths are 88.5° and 50.8°

in October and July, respectively. At respective tilts of 0 and 45°, the collector remains approximately orthogonal to the direction of the solar radiation and receives the maximum amount of irradiation. High irradiation makes it possible to obtain a greater quantity of desorbed adsorbate. Thus, the amount of fluid cycled is high and, accordingly, that of the cooling production. In addition, we note that the SCOP in June (figure 2b) is higher than the SCOP in October (figure 2a). Indeed, in June the machine used less solar energy than in October to produce almost the same refrigerating power. This gives a high ratio in equation 8 and indicates a higher performance of the machine in June than in October.

### 3.2 Effect of collector orientation

Figure 3 shows, on October 21<sup>st</sup>, the effect of collector orientation on the received solar radiation and the times of the heating phases of the cycle. The instantaneous received solar radiation (continuous lines) and the start and end times of the corresponding phase 1 and phase 2 (dashed lines) are plotted for collector orientations of 0° (red lines) and -105° (blue lines); the tilt angle being 10°. It is observed that the curve of the solar radiation received by a collector oriented at -105° is slightly to the right with respect to that received at 0°. This indicates a higher irradiation during the afternoon for a collector oriented at -105° than that oriented at 0°. In terms of times, the two heating phases of the cycle start at 6:00 a.m. and end at different times. Phase 1 and phase 2 end at 8:54 a.m. and 4:54 p.m., respectively for a collector oriented at 0°, and at 9:06 a.m. and 6:00 p.m. for an orientation of -105°.

The analysis shows that phase 2 lasts longer than phase 1. In fact, phase 2 lasts about four to six hours while phase 1 is about three hours. The reason for this is that during phase 1, heating is only used to increase the temperature and pressure of the bed, while during phase 2, it is used to both raise the temperature and to desorb the adsorbate in the bed. On the other side, orienting the collector from 0° to -105° increases the duration of the phases, particularly that of phase 2. In fact, phase 1 and phase 2 increase by 0.2 hour and 1.9 hours, respectively. The duration of phase 2 increases much more than that of phase 1. It is because the overage of solar radiation received under the effect of the orientation at -105 is used further by phase 2 to continue heating the bed.

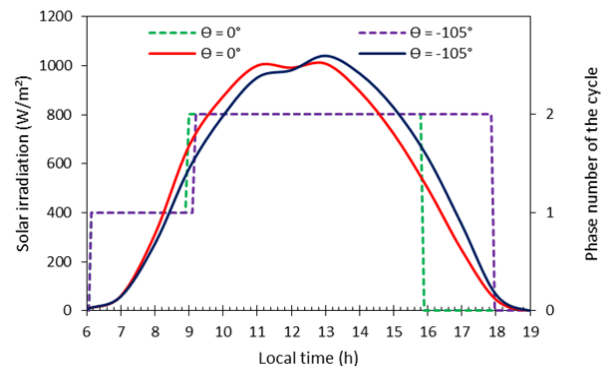


**Fig. 3.** Global solar radiation (continuous line) and phase time (dashed line) of the cycle for two different orientations  $\Theta$  of the solar collector on October 21<sup>st</sup>.

Figure 4 show the effects of the collector orientation on the SCP and the SCOP. In figure 4a the collector was inclined by 45° and oriented from +30° (eastward) to -30° (westward) in increments of 10°, on June 21<sup>st</sup>. The results show that SCP increases until reaching a maximum value of 2.88 W/kg before decreasing. The optimal orientation value is -4.5°.

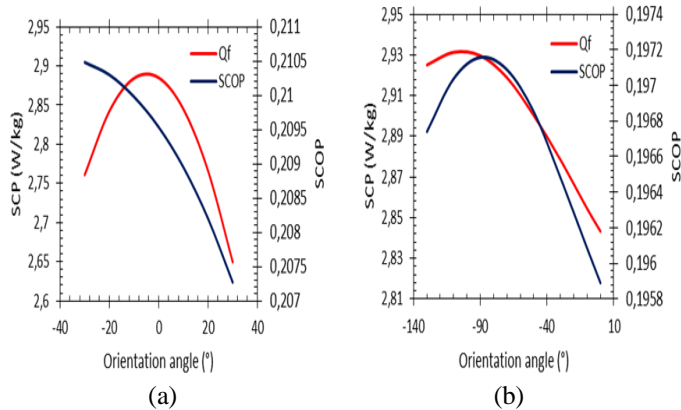


**Fig. 4.** Effect of collector orientation on SCP and the SCOP on (a) June 21<sup>st</sup> and (b) October 21<sup>st</sup>

Between 0° and this optimal orientation value, the SCP and the SCOP increase by 0.22% each. In figure 4b, the collector was inclined by 10° and oriented from 0° (North) to -130° (westward), on October 21<sup>st</sup>. We observe that the SCP and the SCOP increase simultaneously and reach maximum values before decreasing. The maximum values are 2.93 W/kg and 0.197, respectively, and are obtained for optimal orientation values of -105° and -85°. Between 0° and these respective optimal values, the SCP and the SCOP increase by 3.1% and 0.65%, respectively.

These results show that the maximum cooling production and SCOP are obtained for angles of orientation of the collector between 0 and -180°, otherwise stated in the direction of sunset. Indeed, according to the analysis of results of figure 4, the overage of the heating time is used to desorb more adsorbate and

increase the mass of cycled adsorbate. Consequently, we observed increases of the SCP and the SCOP in figure 5.

#### IV. Conclusion

The cooling production and the solar performance of the system were analyzed as a function of the tilt and orientation of the collector. There exists an optimum collector tilt and orientation according to the day. The collector orientation has an influence on the cold production and the system performance.

#### References

- i. W. Chekirou et al., *Dynamic modelling and simulation of the tubular adsorber of a solid adsorption machine powered by solar energy*, *Int. Journal of Refrigeration*. 39 (2014) 137-151
- ii. G. M. Tashtoush et al., *Thermal design of parabolic solar concentrator adsorption refrigeration system*, *Applied Solar Energy*, November 2010, 46, 3, 212–223
- iii. A. Al Mers et al., *Optimal design study of cylindrical finned reactor for solar adsorption cooling machine working with activated carbon–ammonia pair*, *Applied Thermal Engineering* 26 (2006) 1866–1875
- iv. K.C. A. Alam et al., *Adsorption cooling driven by solar collector: A case study for Tokyo solar data*, *Applied Thermal Engineering* 50 (2013) 1603-1609
- v. A.A.A. Qasem et al., *Thermal analysis and modeling study of an activated carbon solar adsorption icemaker: Dhahran case study*, *Energy Conversion and Management* 100 (2015) 310–323
- vi. A. Allouhi et al., *Performance evaluation of solar adsorption cooling systems for vaccine preservation in Sub-Saharan Africa*, *Applied Energy* 170 (2016) 232–241
- vii. M.Pons et al., *Design of an experimental solar powered, solid adsorption ice maker*. *ASME J. Sol. Energ. Eng.* 1986. 108, 332-337.
- viii. J.A. Duffie et al., *Solar Energy Thermal Process*. John Wiley and Sons, INC. 1974
- ix. NASA, *Time series of solar radiation data from the HelioClim-3 database for free*, <http://www.soda-pro.com/web-services/radiation/helioclim-3-for-free>
- x. NASA, *The Modern-Era Retrospective analysis for Research and Applications (MERRA)*, <http://www.soda-pro.com/web-services/meteo-data/merra>